A Global Data Record of Daily Landscape Freeze/Thaw status

Version 5.1

Contact Information:

Youngwook Kim, John S. Kimball, Jinyang Du, and Tobias Kundig

Numerical Terradynamic Simulation Group (NTSG)

The University of Montana

Missoula MT, 59812

Email: john.kimball@umontana.edu; youngwook.kim@umontana.edu;

jinyang.du@umontana.edu; tobias.kundig@umontana.edu

Project URL: http://freezethaw.ntsg.umt.edu/

Release date: 2023-03-31

The following reference should be used to cite these data:

Kim, Y., J. S. Kimball, J. Du, and J. Glassy. 2023. MEaSUREs Global Record of Daily Landscape Freeze/Thaw Status, Version 051 [1979 to 2021]. Boulder Colorado USA: National Snow and Ice Data Center. Digital media (http://dx.doi.org/10.5067/MEASURES/CRYOSPHERE/nsidc-0477.004).

The following peer-reviewed citation provides a detailed description of the FT-ESDR algorithms, accuracy and performance, and science applications:

Kim, Y., J. S. Kimball, J. Glassy, and J. Du. (2017). An Extended Global Earth System Data Record on Daily Landscape Freeze-Thaw Determined from Satellite Passive Microwave Remote Sensing, *Earth System Science Data*, 9 (1), 133-147.

Contents:

I. Introduction:

This document describes a global data record of daily landscape Freeze/Thaw (FT) status derived from satellite passive microwave remote sensing. The FT state parameter quantifies the predominant frozen or non-frozen state of the landscape and is closely linked to changes in the surface energy budget and evapotranspiration (Kim et al., 2018; Zhang et al. 2011), vegetation growth and phenology (Kim et al., 2014b, 2020), snowmelt dynamics (Kim et al., 2015), permafrost extent and stability (Park et al., 2016), wildlife habitat conditions (Zhu et al. 2019), terrestrial carbon budgets and land-atmosphere trace gas exchange (Kim et al., 2014a). Satellite microwave remote sensing is well suited for global FT monitoring due to its relative insensitivity to atmospheric contamination and solar illumination effects, and strong microwave sensitivity to changes in surface dielectric properties between frozen and non-frozen conditions.

II. Data description

The current FT Earth System Data Record (FT-ESDR) was primarily derived using similar calibrated overlapping daily [morning (AM) and afternoon (PM) overpass] radiometric brightness temperature (T_b) measurements at 37 GHz (V-pol) frequency from the Scanning

Multichannel Microwave Radiometer (SMMR), Special Sensor Microwave Imager (SSM/I) and SSM/I Sounder (SSMIS) sensor series. The resulting FT-ESDR represents a consistent, daily FT global record that extends over a 43 year (1979 to 2021) observation period, ensuring cross-sensor consistency through pixel-wise adjustment of the SMMR T_b record based on empirical analyses of overlapping SMMR and SSM/I T_b measurements (Kim et al. 2012). In a similar way, empirical calibrations between overlapping SSM/I and Advanced Microwave Scanning Radiometer 2 (AMSR) T_b measurements was applied to enable FT continuity beyond data year 2020 because the SSM/I Pathfinder T_b record previously used for FT-ESDR production was retired and is no longer available after 2020 (Armstrong et al., 2012).

The SMMR, SSM/I(S) and AMSR components of the FT-ESDR are fully compatible, with similar T_b frequency FT retrievals, consistent projection and product formats, and extending over the same global domain. Calibrated, overlapping T_b data records from SMMR (Knowles et al. 2000), SSM/I and SSMIS (RSS V.7, Armstrong et al. 1998), and AMSR were used to assemble the FT-ESDR. The AMSR L1R swath T_b data (Imaoka et al., 2012) used for FT-ESDR production were first re-projected to the 25-km global EASE-Grid 1.0 projection format using an Inverse Distance Squared spatial interpolation approach following previously established methods (Armstrong and Brodzik, 1995; Du et al., 2014). Detailed descriptions of the FT-ESDR methods, algorithm performance and product accuracy are provided by Kim et al. (2017a).

The FT-ESDR is intended to have sufficient accuracy, resolution, and coverage to resolve physical processes linking Earth's water, energy and carbon cycles. The product is designed to determine the FT status of the composite landscape vegetation-snow-soil medium to a sufficient level to characterize the frozen temperature constraints to surface water mobility, vegetation productivity, ecosystem respiration and land-atmosphere carbon (CO_2) fluxes. The FT-ESDR utilizes a daily binary FT state classification on a per grid-cell basis, posted to a global 25km resolution Earth grid. The FT classification algorithm uses a temporal change detection of radiometric T_b time-series that identify FT transition sequences by exploiting the dynamic temporal T_b response to differences in the aggregate landscape dielectric constant that occur as the landscape transitions between predominantly frozen and non-frozen conditions (McDonald and Kimball 2005; Kim et al., 2011, 2012). Satellite ascending and descending orbital data time

3

series are processed separately to produce information on morning (AM), afternoon (PM) and composite daily FT conditions (CO). Additional variables distinguished by the FT-ESDR include transitional (AM frozen and PM thawed) or inverse transitional (AM thawed and PM frozen) conditions. **Table 2** describes the file encoding of FT-ESDR pixel values corresponding to frozen, thawed, and transitional conditions. The FT-ESDR global domain encompasses all land areas affected by seasonal frozen temperatures, including urban, barren land, snow-ice and open water body dominant grid cells (Kim et al., 2017a).

The FT-ESDR data are available for public access via FTP download through the FT-ESDR project web site (http://www.ntsg.umt.edu/freeze-thaw/) and NTSG HTTP Data Service (http://files.ntsg.umt.edu/data/FT_V5/), and through the NASA DAAC at the National Snow and Ice Data Center (https://nsidc.org/data/nsidc-0477); these data include a variety of file formats including HDF5 and searchable metadata. The FT-ESDR is projected in a global cylindrical Equal-Area Scalable Earth (EASE) grid, Version 1 format (Brodzik and Armstrong 2002) consistent with the format of the underlying SMMR, SSM/I(S) and AMSR global T_b records used as primary inputs for the FT classification.

III. FT-ESDR version 5.1 changes from prior releases

The FT-ESDR Version 5.1 product effectively replaces earlier product releases. The Version 5.1 product contains the following changes from earlier product versions (V5.0 and V4.0), which are designed to improve product coverage, consistency, and performance:

- V5.1: A longer FT data record is represented, extending from 1979 to 2021 (43-years). Since the SSM/I Pathfinder T_b record (Armstrong et al., 2012) previously used for the FT-ESDR ceased production after 2020, FT continuity was enabled using similar frequency (36.5V GHz) AMSR T_b records calibrated to the SSM/I T_b baseline using previously established methods (Kim et al, 2012). To ensure consistency of the long-term T_b and FT records, global calibration of overlapping T_b records from AMSR and SSM/I for data year 2020 was performed for land areas where the open water fraction is less than 0.5.

- V5.1: A separate global FT product stream derived from calibrated AMSR-E and AMSR2 36.5V GHz T_b data spanning the 2002-2020 period is no longer included in the FT-ESDR archive. However, AMSR is used for FT-ESDR production after data year 2020. Users can also access AMSR FT data from the associated Northern Hemisphere Polar Enhanced Resolution (PER) FT product (Kim et al. 2021), or as a global daily frozen flag from the AMSR Land Parameter Data Record (Du et al. 2021).

- V5.0: A modified seasonal threshold algorithm (MSTA) is used for the FT classification where MSTA T_b reference FT conditions are calibrated annually for each pixel using ERA5 (Hersbach et al., 2018) daily surface air temperature (SAT) records;

- V5.0: Over global permanent snow/ice regions, a constant threshold was applied to determine the FT state when the correlation (r-value) between ERA5 SAT and brightness temperature (Tb) is low (absolute value of r < 0.5). The constant Tb threshold used to distinguish FT events was determined annually using mean Tb threshold values derived from pixels with higher correlation (absolute value of r > 0.5) between SSM/I Tb and ERA5 SAT. In addition, diurnal amplitude variation (DAV) of Tb from ascending and descending orbital overpass retrievals was applied as an additional step to confirm thaw condition for the PM overpass only.

IV. FT-ESDR accuracy and performance

The Version 5.1 FT-ESDR release is developed by merging similar vertically (V) polarized, 37 and 36.5 GHz T_b records from SMMR, SSM/I(S), and AMSR, and applying similar protocols used to construct earlier FT-ESDR product versions (Kim et el. 2011, 2012, 2014c). The FT-ESDR extends from 1979 to 2021 over a global classification domain and has been verified against a range of other independent FT metrics, including daily surface air temperature (SAT) measurements from global weather stations, *in situ* lake and river ice phenology records, and satellite observations of Greenland surface ice melt (Kim et al., 2017a). The FT-ESDR product accuracy is primarily assessed in relation to daily SAT maximum (SAT_{max}) and minimum (SAT_{min}) values from the global WMO weather station network (4262±870 [temporal-SD]

stations). Daily SAT_{min} and SAT_{max} records for the selected stations were used to define daily frozen (SAT ≤ 0 °C) and non-frozen (SAT >0 °C) states and compared with the respective AM and PM FT-ESDR products. The FT classification agreement was assessed through grid-cell-to-point comparisons between WMO daily SAT measurements and overlying FT-ESDR results (Kim et al., 2017). Mean annual FT spatial classification accuracies are approximately 90.9 ±1.6 [inter-annual SD] and 85.2 ±1.8 [inter-annual SD] percent for respective FT-ESDR PM and AM retrievals over the global domain and long-term record. The FT-ESDR classification accuracy shows strong seasonal and annual variability, and is generally lower during active FT transition periods when spatial heterogeneity in landscape FT processes is maximized in relation to the relatively coarse (~25-km) satellite footprint (Kim et al. 2017a). Global daily FT spatial classification accuracy is defined for each product daily granule from pixel-wise comparisons of FT classification accuracy in relation to co-located global weather station network daily air temperature (SAT_{min}, SAT_{max}) measurements (Kim et al. 2017a); spatial classification accuracy is expressed as the proportion of global stations where the daily FT classification is consistent with station SAT measurement based FT estimates. Other data quality (QA) metrics are included that provide more spatially explicit information on algorithm performance, including potential negative impacts from open water cover, terrain complexity, length of FT transitional season, and MSTA FT threshold uncertainty influencing mean annual classification accuracy. Additional quality control (QC) flags identify other factors potentially affecting FT classification accuracy. The QC flags are spatially and temporally dynamic, and assigned on a per grid-cell basis to denote missing satellite T_b records that are subsequently gap-filled through temporal interpolation of adjacent successful T_b retrievals prior to the FT classification. The QC flags also distinguish grid cells with large fractional open water areas (fw>0.20) and extreme elevation gradients (>300m), and days with identified large precipitation events (Ferraro et al., 1996).

V. FT algorithms:

The FT-ESDR classification involves a modified seasonal threshold algorithm approach (MSTA) with radiometric T_b time-series that identify FT transition sequences by exploiting the dynamic T_b temporal response to differences in the aggregate landscape dielectric constant that occur as the landscape transitions between predominantly frozen and non-frozen conditions.

These techniques are well-suited for resolving daily FT state dynamics rather than single events or seasonally dominant transitions (Kim et al. 2011). The Version 5.1 product uses the MSTA to classify daily (AM and PM) FT status from calibrated SMMR, SSM/I(S), and AMSR2 T_b records. The MSTA FT threshold was defined annually using an empirical linear regression relationship between the satellite T_b retrievals and daily ERA5 SAT estimates established for each grid cell. The FT thresholds were derived separately for the satellite T_b time series from AM and PM overpasses and using corresponding daily SAT minimum (SAT_{min}) and maximum (SAT_{max}) values. Larger weighting of SAT values closer to 0°C was used in selecting the corresponding T_b based FT threshold for each grid cell; weighting of the SAT and T_b regression relationship was derived using a cosine function within a temperature range extending from -60.0°C to 30.0°C and representing 99 percent of the SAT frequency distribution defined from the SAT global climatology (Kim et al., 2017a). An advantage of the MSTA relative to an earlier seasonal threshold algorithm (STA) based FT classification (Kim et al. 2011) is that the T_b threshold selection does not depend on frozen and non-frozen reference states derived by averaging T_b measurements over respective winter and summer periods, and is less sensitive to T_b data gaps during these reference periods.

Over permanent snow/ice regions, a constant threshold was applied to determine the FT state when the correlation between ERA5 SAT and brightness temperature (Tb) is low (absolute value of $r <= 0.5$). The constant threshold was determined annually using mean threshold values derived from the values with higher correlation (absolute value of $r > 0.5$) between SSM/I Tb and ERA5 SAT. The diurnal amplitude variation (DAV) of AM and PM overpass Tb retrievals for a grid cell was used as a second criteria to confirm the thaw condition for the PM overpass only. A 10 degree Kelvin Tb amplitude was used as the DAV threshold (Ramage et al., 2006; Mioduszewski et al., 2014) for lower correlation grid cells. When the absolute value of DAV is more than 10 degrees Kelvin, the FT state is confirmed as thawed.

VI. Ancillary data used for the FT-ESDR

We used daily SAT records from the ECMWF ERA5 global model reanalysis for pixel-wise annual calibration the MSTA FT thresholds. The global reanalysis data were also used to define the global FT-ESDR domain (**Figure 1**) using a simple SAT driven bioclimatic index (Kim et al.

2011) that identified all land areas where seasonally frozen temperatures are a significant constraint to ecosystem processes and land surface water mobility (Kim et al., 2017a).
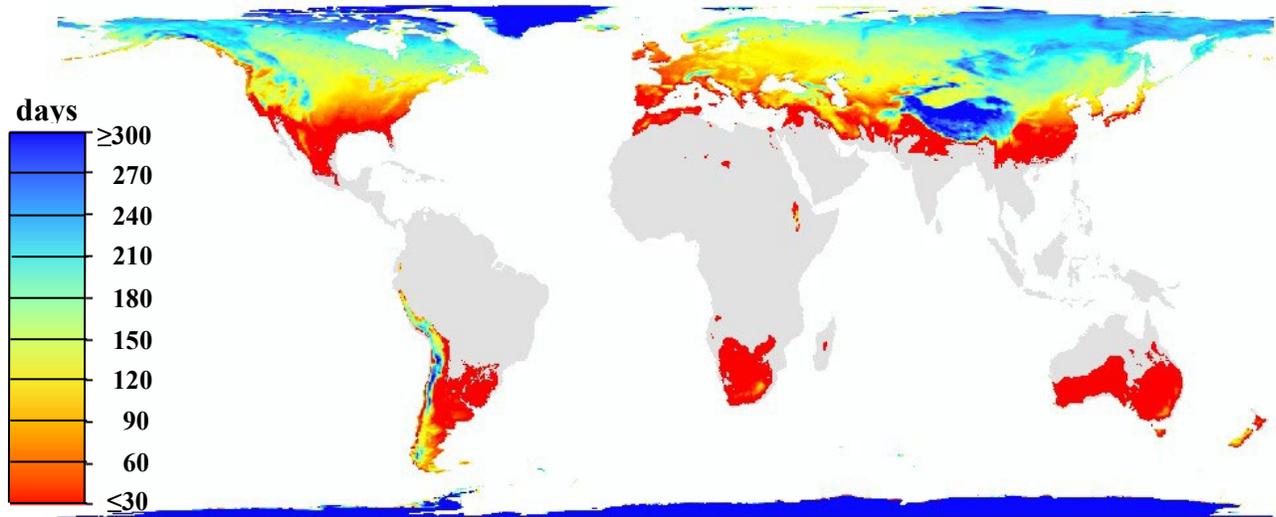

Figure 1: *Mean annual frozen season (frozen or transitional status;1979-2020) over the global FT-ESDR domain; white and grey colors denote respective open water bodies and land areas outside of the FT-ESDR domain.*

Independent daily SAT observations from global in situ WMO weather station measurements were used for verification of FT-ESDR daily accuracy. A simple zero degree Celsius temperature threshold was used to classify frozen and non-frozen temperatures from the SAT measurements; these results were then compared against the FT-ESDR daily classification results from the overlying grid cell. The resulting global FT spatial classification accuracy from all WMO stations was then summarized on a daily basis.

A global QA map is defined for each year of record and provides a discrete, grid cell-wise indicator of relative FT-ESDR quality that accounts for potential negative impacts from open water cover, terrain complexity, length of FT transitional season, and MSTA FT threshold uncertainty influencing mean annual FT classification accuracy indicated from the WMO station comparisons. The resulting annual QA map for selected year 2012 is presented in **Figure 2** and shows regions of relative high to low quality. The QA values were stratified into a smaller set of discrete categories ranging from low (estimated mean annual FT classification accuracy < 70%) to best (> 90%) quality. Mean proportions of the four QA categories encompass 54.1% (best),

36.0% (good; 80-90% agreement), 6.6% (moderate; 70-80% agreement), and 3.3% (low; <70% agreement) of the global FT-ESDR domain for 2012.
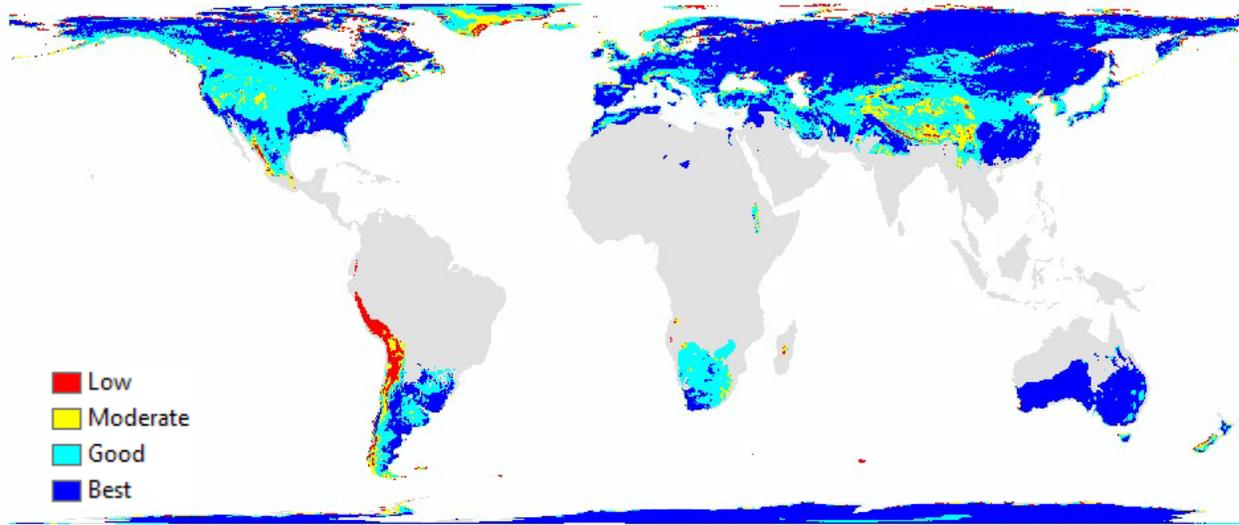
Figure 2: FT-ESDR annual quality assurance (QA) map for selected year of record 2012, aggregated into low (estimated mean annual spatial classification agreement < 70%), moderate (70-80%), good (80-90%) and best (>90%) relative quality categories. Land areas outside of the FT-ESDR domain are denoted by grey shading.

VII. Hierarchical data archive structure and available software tools:

The University of Montana FT-ESDR data are publicly accessible through the online NTSG FTP service. The data are organized in a hierarchical file structure by sensor type and year of record. The FT-ESDR V5.1 data and associated file structure are also available in a set of compressed "tar" archive files to facilitate downloading of the complete record. The tar archives consist of the following files as documented in **Table 1** below. The data includes global daily FT classification files in HDF5 and GeoTIFF formats; daily FT accuracy and annual QA maps, and supporting FT-ESDR documentation and software tools. The FT-ESDR data, made up of GeoTIFF, GIF and HDF5 file formats, are stored in three folders DAILY_GEOTIFF, DAILY_GIF and DAILY_HDF5, respectively. The Quality Assurance and Accuracy HDF5 files are in the QA_ACCURACY folder. Within each folder, the daily FT or quality flag data are organized by sensor names (AMSR, SMMR and SSMI) and then by year of record.

Table 1. Tar archive files encompassing the FT-ESDR (v5.1) release.

9

FT-ESDR v5.1 File Summary	
[1]Directory	Summary of Contents
DAILY_HDF5	Multi-year record of global daily HDF5 science granules
DAILY_GIF	Multi-year record of global daily browse images (GIF format) for quick visual evaluation
QA_ACCURACY	Daily FT-ESDR mean global classification accuracy (%) and annual QA metadata in HDF5 file formats. The value -9999 refers to no data.
TAR_ARCHIVES	Compressed tar file (*.tar.gz) archive of the FT-ESDR file hierarchy intended to facilitate distribution and network transfer of the complete data record
MD5	MD5 checksum hash signatures for each FT file in the collection
DOC_V5.1	FT-ESDR database documentation files
TOOLS	File viewing software, including Panoply (v3.1.5) and HDFView (v2.8) for HDF5 (on MacOS, windows, Linux platforms)

[1]*Note that within a given directory tree such as DAILY_HDF5, where there are two subtrees for the different sensor FT records ("./AMSR", and "./SMMR_SSMI"), a series of year-wise directories (2002-2021 or 1979-2021) occur below each of these.*

Two commonly available software tools (HDFView and Panoply) are available through the FT-ESDR project and are routinely used with the predominant HDF5 and GeoTIFF file formats of the FT-ESDR. Other tool environments are also commonly used, such as ArcGIS, IDL/ENVI, MatLAB, "R" (rhdf), and various Python implementations (e.g. h5py and GDAL for Python) that support user developed code. Users of the HDF Groups hdfview utility should consult the following URL for additional information regarding their specific platform since there are distinctions in the binary distributions offered based on the user's operating system (e.g. whether it is 32 or 64 bit, etc.): https://support.hdfgroup.org/products/java/release/download.html

VIII. Data format and file naming convention:

Daily FT Status

The FT data are stored in unsigned 8-bit integer data format as follows, shown with the GIF browse image color mapping scheme used (**Table 2**).

Table 2. FT-ESDR 8-bit integer data identifiers, with associated RGB colors used in the GIF browse images.

Classification	FT DN	Browse Image Color Table		
		R	G	B
Frozen (AM/PM frozen)	0	000	000	255
Thawed (AM/PM thawed)	1	255	000	000
Transitional (AM frozen and PM thawed)	2	168	168	000
Inverse Transitional (PM frozen and AM thawed)	3	076	230	000
No FT status available	252	250	250	250
Non-cold constraint area	253	255	255	255
100% open water	254	204	255	255
Fill value	255	255	255	255

Each FT-ESDR grid cell is projected in a global EASE-Grid 1.0 format (Armstrong & Brodzik, 1995; Brodzik and Armstrong 2002) at 25km spatial resolution, with 1383 columns and 586 rows consisting of 8-bit byte data type for a total of 810,438 pixels per daily data product. An ESRI geographic projection file is included with the GeoTIFF files to aid in viewing the data in the ArcMap and ArcGIS software environment. The projection file is available through the NTSG HTTP Data Service (http://files.ntsg.umt.edu/data/FT_ESDR/DOCS_v5/NSIDC_EASE_GRID_GLOBAL_FT_Sample.prj). The geographical range of the FT-ESDR product is global, extending from -179.9999º to 179.9999 º longitude and from -86.7167º to 86.7167º latitude.

The FT-ESDR includes dynamic quality control (QC) flags that are identified within an 8-bit character field for each grid cell as summarized below (**Table 3**). The first QC bit flag value (0) identifies whether actual T_b retrievals or interpolated T_b values were used for the daily FT classification. The second bit flag (1) denotes cells with a large spatial fraction of open water cover (fw > 20%), which is consistent with the fw threshold used for prior FT-ESDR releases (Kim et al., 2011). The third bit flag (2) denotes grid cells with a large elevation gradient (>300m), defined as the spatial standard deviation of the elevation distribution within each 25-km FT-ESDR grid cell, and derived from a global digital elevation map. The fourth bit flag (3)

identifies large daily precipitation events occurring within a grid cell, and defined using a T_b threshold approach (Ferraro et al., 1996).

Table 3. Summary of FT-ESDR grid cell-wise Quality Control (QC) bit flags.

QC bit	Description (flagged=1, non-flagged=0)
0	flagged as 1 in case of interpolated T_b, otherwise set to 0
1	flagged as 1 in case of large open water fraction (>20%), otherwise set to 0
2	flagged as 1 in case of large elevation gradient (>300m), otherwise set to 0
3	flagged as 1 in case of large precipitation events, otherwise set to 0
4-7	bits unused

Each daily FT file consists of 3 separate granules, including: morning overpass (AM), afternoon overpass (PM) and combined daily AM and PM (CO) classification results. The FT product naming protocol follows these conventions:

[InstrumentLabel]_[Channel][Polarization]_[OverpassCode]_FT_[Year]_day[DOY].bin

For example, the file "SSMI_37V_CO_FT_2014_day365.bin" represents SSM/I and SSMIS sensor, 37 GHz, vertically polarized T_b based FT classification for composite daily conditions for day (calendar year) 365.

Annual FT Accuracy

Annual accuracy files are available for both AM and PM overpasses. Accuracy is assessed in relation to daily maximum and minimum air temperature measurements from the global WMO weather station network and expressed as the percent of daily FT retrievals per year that are consistent with in situ air temperature measurements. Values stored in the "ft_annual_accuracy" data field are reported in the range of 0.0 to 100.0. The accuracy product naming protocol follows these conventions:

[InstrumentLabel]_[Channel][Polarization]_[OverpassCode]_FT_[Year]_ accuracy.h5

Annual FT Status Quality Assurance

Annual FT Status Quality Assurance (QA) represents a relative index of data quality for each grid cell based on the potential negative impacts from data gaps, open water, terrain complexity, length of FT transitional season, and uncertainty in the FT algorithm threshold. QA values stored

in "ft_annual_QA" data field are reported from 0.0 to 1.0 and categorized as: QA < 0.70 = low; 0.70 < QA < 0.85 = moderate; 0.85 < QA < 0.95 = good; QA > 0.95 = best. Separate files are available for each year in each satellite record. The QA product naming protocol follows these conventions:

[InstrumentLabel]_ global_QA _[Year]_ [OverpassCode].h5

IX. Data Organization and Volume:

The daily FT data is organized in this collection first by sensor label, and then by year, with the AM, PM and CO granules stored in each annual directory. The FT-ESDR file sizes vary depending on the particular format option selected (**Table 4**). The FT-ESDR is also offered as a collection of matching HDF5 granules, which include an embedded FT classification legend, QC flags, production metadata, pixel statistics and frequency counts for the granule, and CF convention style coordinate geolocation variables (cell_lat, cell_lon) to aid viewing. In addition to the primary FT data, detailed product quality information is also provided that includes granule level total mean spatial classification accuracy for the global domain defined on a daily basis (defined from pixel-wise comparisons against co-located global weather station SAT observations), and spatially contiguous relative data quality (QA) maps updated for each annual cycle. The FT-ESDR consists of a total of 71,233 daily global 25km resolution granules, and a total of approximately 20 GB (HDF5 format) for the entire FT-ESDR database. For faster downloading, compressed ("gzip") yearly FT binary files are provided in the "DAILY_TAR_ARCHIVES" directory.

Table 4. FT-ESDR file size summaries for HDF5 files.

Instrument	N. files	Range of Years	HDF5 Files	
			MB	GB
SMMR	8767	1979 – 1986	2470	2.5
SSM/I(S)	38352	1987 – 2020	10815	11

|				
AMSR	1095	2021	311	.311
Totals:	48214	42	13596	13.811

A number of compressed tar archives (**Table 5**) are also available (see DAILY_TAR_ARCHIVES directory) as a convenient method for users to access related collections of the FT- ESDR files. Their names, manifests (table of content files), number of files, and data volume sizes are documented in the table below:

Table 5. FT-ESDR compressed tar file (tar.gz) archives and file sizes available for download.

Tar Archive Name	N. Files	Size
FT_V5.1_HDF5.tar.gz	48217	4.5 GB
FT_V5.1_HDF5_QA_ACC_.tar.gz	178	28 MB
FT_V5.1_GeoTIFF.tar.gz	47162	1.4 GB
FT_V5.1_GIF.tar.gz	44926	2.4 GB

X. Example FT Figures:

The FT-ESDR provides a daily (CO) classification of the predominant landscape frozen or non-frozen status for each grid cell within the global domain (**Figure 3**). Four discrete FT metrics are distinguished from the AM and PM T_b retrievals, including frozen (both AM and PM overpasses), non-frozen (AM and PM), transitional (AM frozen, PM non-frozen) and inverse-transitional (AM non-frozen, PM frozen) states.
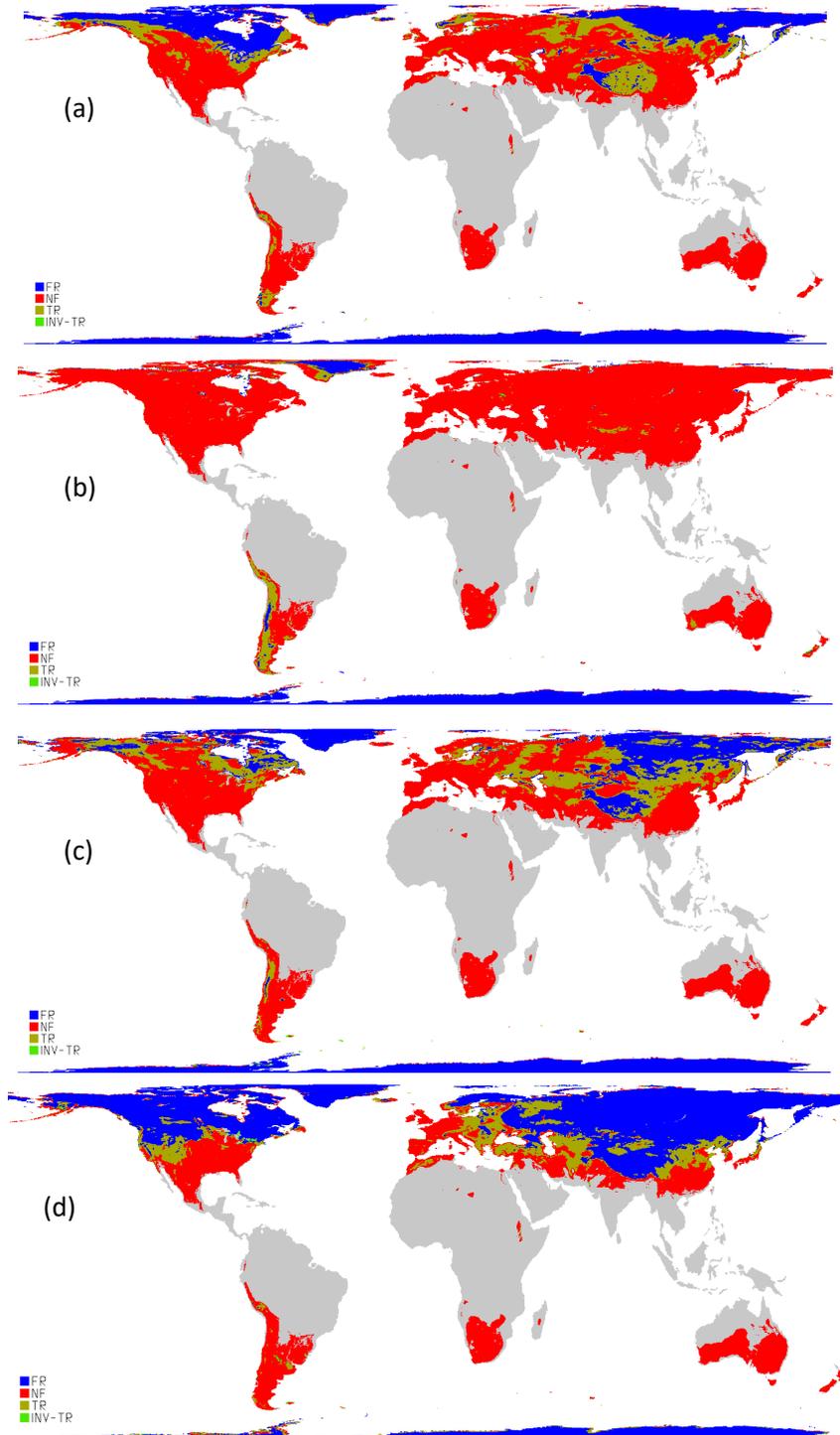
Figure 3*: Daily combined (CO) FT-ESDR classification results for selected year of record 2016,
where: (a) DOY (Day of Year) =100, (b) DOY=200, (c) DOY=300, and (d) DOY=360; white*

and grey colors denote respective open water bodies and land areas outside of the FT-ESDR domain; FR (AM and PM frozen), NF (AM and PM thawed), TR (AM frozen and PM thawed) and INV-TR (AM thawed and PM frozen).

XI. References:

Armstrong, R. L. and M. J. Brodzik. 1995. An Earth-Gridded SSM/I Data Set for Cryosphere Studies and Global Change Monitoring. *Advances in Space Research*. 16, 155-163.

Armstrong, R., K. Knowles, M. Brodzik, and M.A. Hardman, 1998, updated 2012. DMSP SSM/I-SSMIS Pathfinder Daily EASE-Grid Brightness Temperatures. Version 2 [1987-2012]. Boulder, Colorado USA: NASA DAAC at the National Snow and Ice Data Center (http://nsidc.org/data/nsidc-0032.html).

Brodzik, M. J. and R. L. Armstrong. 2002. EASE-Grid: A versatile set of equal-area projections and grids. In M. Goodchild (Ed.), Discrete Global Girds. Santa Barbara, California USA: National Center for Geographic Information and Analysis.

Du, J., J. S. Kimball, L. Jones, Y. Kim, J. Glassy, and J. D. Watts. 2017a. A global satellite environmental data record derived from AMSR-E and AMSR2 microwave Earth observations. *Earth Syst. Sci. Data*, 9, 791–808, 2017. https://doi.org/10.5194/essd-9-791-2017.

Du, J. and J. S. Kimball. (2021). Daily Global Land Parameters Derived from AMSR-E and AMSR2, Version 3 [Data Set]. Boulder, Colorado USA. NASA National Snow and Ice Data Center Distributed Active Archive Center. https://doi.org/10.5067/WPXUQ72A4484.

Du, J., J. S. Kimball, J. Shi, L. A. Jones, S. Wu, R. Sun, and H. Yang. (2014). Inter-calibration of satellite passive microwave land observations from AMSR-E and AMSR2 using overlapping FY3B-MWRI sensor measurements. *Remote Sensing*, 6, 8594-8616.

Ferraro, R. R., F. Weng, N. C. Grody, and A. Basist. (1996). An eight-year (1987-1994) time series of rainfall, clouds, water vapor, snow cover, and sea ice derived from SSM/I measurements. *Bulletin of the American Meteorological Society*, 77(5), 891-905.

Hersbach, H., Bell, B., Berrisford, P., Biavati, G., Horányi, A., Muñoz Sabater, J., Nicolas, J., Peubey, C., Radu, R., Rozum, I., Schepers, D., Simmons, A., Soci, C., Dee, D., Thépaut, J-N. (2018): ERA5 hourly data on single levels from 1979 to present. Copernicus Climate Change Service (C3S) Climate Data Store (CDS).

Imaoka, K.; Takashi, M.; Misako, K.; Marehito, K.; Norimasa, I.; Keizo, N. (2012). Status of AMSR2 instrument on GCOM-W1, earth observing missions and sensors: Development, implementation, and characterization II. Proc. SPIE 2012, 852815, doi:10.1117/12.977774

JAXA. Digital media (https://gcom-w1.jaxa.jp).

Jones, L.A., and J.S. Kimball, 2010, updated 2012. Daily Global Land Surface Parameters Derived from AMSR-E, Version 1.1. Boulder Colorado USA: National Snow and Ice Data Center. Digital media (http://nsidc.org/data/nsidc-0451.html).

Kim Y., Kimball J.S., Parazoo N., Kirchner P. 2020. Diagnosing Environmental Controls on Vegetation Greening and Browning Trends Over Alaska and Northwest Canada Using Complementary Satellite Observations. In: Yang D., Kane D. (eds) Arctic Hydrology, Permafrost and Ecosystems. Springer, doi.org/10.1007/978-3-030-50930-9_20

Kim, Y., J. S. Kimball, J. Du, C. L. B. Schaaf, and P. B. Kirchner. 2018. Quantifying the effects of freeze-thaw transitions and snowpack melt on land surface albedo and energy exchange over Alaska and Western Canada, *Environmental Research Letters*, 13 (7), 1-14

Kim, Y., J. S. Kimball, J. Glassy, and J. Du. 2017a. An Extended Global Earth System Data Record on Daily Landscape Freeze-Thaw Determined from Satellite Passive Microwave Remote Sensing, *Earth System Science Data*, 9 (1), 133-147.

Kim, Y., J. S. Kimball, J. Du, and J. Glassy. (2021). MEaSUREs Polar EASE-Grid 2.0 Daily 6 km Land Freeze/Thaw Status from AMSR-E and AMSR2, Version 2 [Data Set]. Boulder, Colorado USA. NASA National Snow and Ice Data Center Distributed Active Archive Center. https://doi.org/10.5067/BDY2V548E07C.

Kim, Y., J. S. Kimball, J. Du, and J. Glassy. (2021). MEaSUREs Global Record of Daily Landscape Freeze/Thaw Status, Version 5 [Data Set]. Boulder, Colorado USA. NASA National Snow and Ice Data Center Distributed Active Archive Center.

Kim, Y., J. S. Kimball, J. Glassy, and K. C. McDonald. 2017b. MEaSUREs Global Record of Daily Landscape Freeze/Thaw Status, Version 4. [Indicate subset used]. Boulder, Colorado USA. NASA National Snow and Ice Data Center Distributed Active Archive Center. doi: https://doi.org/10.5067/MEASURES/CRYOSPHERE/nsidc-0477.004. [Date Accessed].

Kim, Y., J. S. Kimball, D. A. Robinson, and C. Derksen. 2015. New satellite climate data records indicate strong coupling between recent frozen season changes and snow cover over high northern latitudes. *Environmental Research Letters*, 10, 084004.

Kim, Y., J. S. Kimball, K. Zhang, K. Didan, I. Velicogna, and K. C. McDonald. 2014a. Attribution of divergent northern vegetation growth responses to lengthening non-frozen seasons using satellite optical-NIR and microwave remote sensing, *International Journal of Remote Sensing*, 10.1080/01431161.2014.915595.

Kim, Y., J. S. Kimball, K. Didan, and G. M. Henebry. 2014b. Responses of vegetation growth and productivity to spring climate indicators in the conterminous Unites States derived from satellite remote sensing data fusion. *Agricultural and Forest Meteorology*, 194, 132-143

Kim, Y., J. S. Kimball, J. Glassy, and K. C. McDonald. 2014c. MEaSUREs Global Record of Daily Landscape Freeze/Thaw Status. Version 3. [1979-2011]. Boulder, Colorado USA: NASA DAAC at the National Snow and Ice Data Center. http://dx.doi.org/10.5067/MEASURES/CRYOSPHERE/nsidc-0477.003

Kim, Y., J.S. Kimball, K. Zhang, and K.C. McDonald, 2012. Satellite detection of increasing northern hemisphere non-frozen seasons from 1979 to 2008: Implications for regional vegetation growth. *Remote Sensing of Environment* 121, 472-487.

Kim, Y., J. S. Kimball, K. C. McDonald, and J. Glassy. 2011. Developing a Global Data Record of Daily Landscape Freeze/Thaw Status using Satellite Microwave Remote Sensing. *IEEE Transactions on Geoscience and Remote Sensing*. 49, 3, 949-960.

Knowles, K., M. Savoie, R. Armstrong, and M. Brodzik, 2006, updated 2011. AMSR-E/Aqua Daily EASE-Grid Brightness Temperatures [2002-2011]. Boulder, Colorado USA: NASA DAAC at the National Snow and Ice Data Center (http://nsidc.org/data/nsidc-0301.html).

Knowles, K., E.G. Njoku, R. Armstrong, and M. Brodzik, 2000. Nimbus-7 SMMR Pathfinder Daily EASE-Grid Brightness Temperatures [1979-1987]. Boulder, Colorado USA: NASA DAAC at the National Snow and Ice Data Center (http://nsidc.org/data/nsidc-0071.html).

McDonald, K.C, and J.S. Kimball, 2005. Hydrological application of remote sensing: Freeze-thaw states using both active and passive microwave sensors. Encyclopedia of Hydrological Sciences. Part 5. Remote Sensing. M.G. Anderson and J.J. McDonnell (Eds.), John Wiley & Sons Ltd. DOI:10.1002/0470848944.hsa059a.

Mioduszewski, J. R., A. K. Rennermalm, D. A. Robinson, and T. L. Mote. 2014. Attribution of snowmelt onset in Northern Canada, *J. Geophys. Res. Atmos.*, 119, doi:10.1002/2013JD021024.

Park, H., Y. Kim, and J. S. Kimball. (2016). Widespread permafrost vulnerability and soil active layer increases over the high northern latitudes inferred from satellite remote sensing and process model assessments. *Remote Sensing of Environment*, 175, 349-358.

Ramage, J. M., R. A. McKenney, B. Thorson, P. Maltais and S. E. Kopczynski. 2006. Relationship between passive microwave-derived snowmelt and surface-measured discharge, Wheaton River, Yukon Territory, Canada. *Hydrol. Process*. 20, 689–704

Yang, H., F. Weng, L. Lv, N. Lu, G. Liu, M. Bai, Q. Qian, J. He, H. Xu. (2011) The FengYun-3 microwave radiation imager on-orbit verification. *IEEE Transactions on Geoscience and Remote Sensing*, 49, 4552–4560.

Zhang, K., J.S. Kimball, Y. Kim, and K.C. McDonald, 2011. Changing freeze-thaw seasons in northern high latitudes and associated influences on evapotranspiration. *Hydrological Processes* 25, 4142-4151, DOI:10.1002/hyp.8350.

Zhu, L., A.R. Ives, C. Zhang, Y. Guo, and V.C. Radeloff, 2019. Climate change causes functionally colder winters for snow cover-dependent organisms. *Nature Climate Change* 9, 886-893.